

## Research Article

# Controlling Mechanism of Rock Burst by CO<sub>2</sub> Fracturing Blasting Based on Rock Burst System

Tianwei Lan,<sup>1,2</sup> Chaojun Fan ,<sup>1</sup> Jun Han,<sup>1</sup> Hongwei Zhang,<sup>1</sup> and Jiawei Sun<sup>1</sup>

<sup>1</sup>College of Mining, Liaoning Technical University, Fuxin 123000, China

<sup>2</sup>Key Laboratory of Mining Disaster Prevention and Control, Qingdao 266590, China

Correspondence should be addressed to Chaojun Fan; [chaojunfan@139.com](mailto:chaojunfan@139.com)

Received 27 April 2020; Revised 28 July 2020; Accepted 5 August 2020; Published 27 August 2020

Academic Editor: Caiping Lu

Copyright © 2020 Tianwei Lan et al. This is an open access article distributed under the Creative Commons Attribution License, which permits unrestricted use, distribution, and reproduction in any medium, provided the original work is properly cited.

Rock burst induced by mining is one of the most serious dynamic disasters in the process of coal mining. The mechanism of a rock burst is similar to that of a natural earthquake. It is difficult to accurately predict the “time, space, and strength” of rock burst, but the possibility of rock burst can be predicted based on the results of microseismic monitoring. In this paper, the rock burst system under the tectonic stress field is established based on the practice of coal mining and the result of mine ground crustal stress measurement. According to the magnitude of microseismic monitoring, the amount of the energy and spatial position of the rock burst are determined. Based on the theory of explosion mechanics, aiming at the prevention and control of rock burst in the coal mine, the technique of liquid CO<sub>2</sub> fracturing blasting is put forward. By the experiment of blasting mechanics, the blasting parameters are determined, and the controlling mechanism of rock burst of liquid CO<sub>2</sub> fracturing blasting is revealed. The application of liquid CO<sub>2</sub> fissure blasting technology in the prevention and control of rock burst in Jixian Coal Mine shows that CO<sub>2</sub> fracturing blasting reduces the stress concentration of the rock burst system and transfers energy to the deeper part, and there is no open fire in the blasting. It is a new, safe, and efficient method to prevent and control rock burst, which can be applied widely.

## 1. Introduction

Rock burst is one of the most serious dynamic disasters in coal mining. Both rock burst and natural earthquake are dynamic disasters caused by the crack and instability of crustal rock mass, resulting in the release of energy. The occurrence mechanisms of the two are similar and they are difficult to be predicted [1–4]. The research on the mechanism of rock burst has always been an unsolved scientific problem that has been discussed for a long time in the fields of mining engineering and rock mechanics [5–10]. The application of CT scanning, 3D printing, big data, cloud computing, Internet of things, and other emerging technologies in the study of coal mine rock burst has become a hot topic in mining research [11–14]. The monitoring and warning methods of rock burst mainly include microseismic monitoring method, electromagnetic radiation method, AE method, mining stress monitoring method, and drilling cuttings method. Through the analysis of monitoring data,

the possibility of rock burst can be predicted, but the accuracy still needs to be further improved [15–19]. For the prevention of rock burst, there are two aspects: regional prevention and local risk relief, including protection layer mining, borehole pressure relief, coal seam water injection, pressure relief blasting, liquid CO<sub>2</sub> fracturing blasting, hydraulic fracturing, and other methods [20–23]. Through the implementation of risk relief measures, the risk of rock burst is reduced. But the exact location of the rock burst cannot be determined; it leads to the heavy workload and material consumption. If the structure and energy characteristics of coal and rock mass can be predicted and preventive measures can be taken according to the predicted results, the prevention level of rock burst will be improved and the cost of risk relief will be reduced.

The gestation and generation of rock burst can be affected by the stress concentration degree and energy storage size of the regional coal-rock mass structure system, and the coal-rock mass system should have a certain scale range

[24, 25]. In order to study the structure system and energy characteristics of rock mass under rock burst, a rock burst system based on the tectonic stress field is established. The energy magnitude and spatial location of rock burst system are determined by microseismic monitoring technology. Based on the established rock burst system, the liquid CO<sub>2</sub> fracturing blasting technology is put forward. The practice of preventing and controlling rock burst in coal mine shows that the CO<sub>2</sub> fracturing blasting reduces the stress concentration of the rock burst system and transfers the energy to the deeper part. It is a new, safe, and efficient technology to prevent rock burst.

## 2. Analysis of Energy in Rock Burst System

**2.1. Establishment of Rock Burst System.** The complexity of rock burst is related to the heterogeneity, anisotropy, and diversity of influencing factors of the structure system of coal and rock mass. The stress and energy of coal and rock mass system are the basic conditions, and the mining engineering activities are the induced conditions. More than 85% of the energy causing rock burst comes from surrounding rock. The coal mainly provides the medium condition for rock burst. The space of energy storage-exchange-release of coal and rock mass system with rock burst should have a certain scale, which cannot be infinitely great or infinitely small, and should be related to the structure, stress, and energy level in the coal and rock mass system. A model of rock burst system, which reflects the relation of the coal and rock mass system and rock burst, is established. The shape of the model is assumed to be spherical, hereinafter referred to as the rock burst system (Figure 1).

**2.2. Analysis of Energy in Rock Burst System.** According to the theory of elasticity, a representative element of rock mass at the depth  $H$  in the crustal rock mass is subjected to three-dimensional stress, and the unit body is in the state of elastic deformation (Figure 2). The elastic energy of unit volume accumulation under in situ stress field can be expressed by the following formula:

$$U_0 = \frac{1}{2E} [\sigma_1^2 + \sigma_2^2 + \sigma_3^2 - 2\mu(\sigma_1\sigma_2 + \sigma_2\sigma_3 + \sigma_1\sigma_3)], \quad (1)$$

where  $U_0$  represents elastic energy accumulated in unit volume, J;  $\sigma_1$ ,  $\sigma_2$ , and  $\sigma_3$  represent principal stress in three directions of any unit, MPa;  $E$  represents modulus of elasticity, MPa;  $\mu$  represents Poisson's ratio.

Then, the energy for the spherical rock burst system can be expressed:

$$U = \frac{1}{2E} [\sigma_1^2 + \sigma_2^2 + \sigma_3^2 - 2\mu(\sigma_1\sigma_2 + \sigma_2\sigma_3 + \sigma_1\sigma_3)] \frac{4}{3} \pi R^3, \quad (2)$$

where  $U$  represents the energy of rock burst system, J;  $R$  represents the radius of rock burst system, m.

According to the in situ stress measurement results of some rock burst mines in China, the stress fields in most (almost all) areas are horizontal compressive tectonic stress

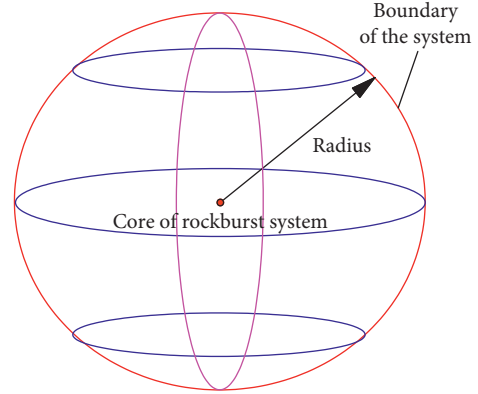


FIGURE 1: Schematic diagram of "spherical" type rock burst system.

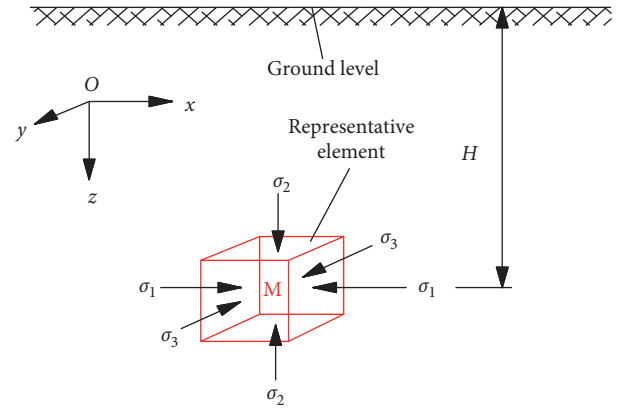


FIGURE 2: Representative element under the action of three-dimensional stress.

fields. The change of maximum principal stress direction and magnitude in most parts of China is due to the collision of the Chinese mainland plate by the India plate and Eurasian plate and the subduction of the eastern Pacific plate and the Philippines plate to Eurasia. In the vast majority of areas, the in situ stress is a three-dimensional unequal compressive stress field dominated by horizontal stress. The magnitude and direction of the three principal stresses vary with space and time, so they are unstable stress fields. The measured data show that the vertical stress is basically equal to the weight of overlying strata. The deviation between the vertical stress direction and the vertical direction is generally no more than 20°. The measured data show that there are two principal stresses in the horizontal or nearly horizontal plane in most (almost all) regions, and the angle between the two principal stresses and the horizontal plane is generally no more than 30°.

The dip angles of the maximum and minimum principal stresses  $\sigma_1$  and  $\sigma_3$  are near horizontal direction. The maximum horizontal stress  $\sigma_1$  is generally larger than the vertical stress  $\sigma_2$ , and there are certain linear relationships between  $\sigma_1$ ,  $\sigma_2$ , and  $\sigma_3$  and self-weight stress  $\gamma H$ , and they are usually  $\sigma_1 \approx 2\gamma H$ ,  $\sigma_2 \approx \gamma H$ , and  $\sigma_3 \approx 0.7\gamma H$ . The energy of rock burst system related to self-weight stress can be obtained by substituting them into formula (2).

$$U = \frac{2\pi}{3E} (5.49 - 8.2\mu)\gamma^2 H^2 R^3. \quad (3)$$

**2.3. Analysis of Scale in Rock Burst System.** When the energy stored in the rock burst system reaches the critical state of the energy required for the occurrence of the rock burst, mining engineering activities induce the instability of the rock burst system, and the instantaneous release of energy causes the rock burst. So, the rock burst is a nonlinear dynamic process of energy accumulation in steady state and energy release in a nonsteady state in the deformation process of rock burst system.

The energy of rock burst  $\Delta U$  is provided by the rock burst system, which is usually determined by the difference between the energy of tectonic stress field  $U_G$  and the energy of gravity stress field  $U_Z$ . By calculation,

$$\begin{cases} U_Z = \frac{2\pi}{3E} \left( \frac{1-2\mu^2-\mu}{1-\mu} \right) \gamma^2 H^2 R^3, \\ U_G = \frac{2\pi}{3E} (5.49 - 8.2\mu) \gamma^2 H^2 R^3. \end{cases} \quad (4)$$

Then,

$$\Delta U = U_G - U_Z = \frac{2\pi(10.2\mu^2 - 12.69\mu + 4.49)\gamma^2 H^2 R^3}{3E(1-\mu)}. \quad (5)$$

Therefore, we can obtain the radius of the rock burst system as

$$R = \sqrt[3]{\frac{3E(1-\mu)\Delta U}{2\pi(10.2\mu^2 - 12.69\mu + 4.49)\gamma^2 H^2}}. \quad (6)$$

Rock burst and natural earthquake are both dynamic disasters caused by the crack and instability of crustal rock mass. It can also be considered that rock burst is an earthquake induced by mining. In seismology, the energy to produce an earthquake can be determined by Gutenberg's and Kanamori's empirical formulas of energy magnitude. The principle of microseismic monitoring is similar to that of earthquake prediction and has been widely used in the monitoring of rock burst in coal mines. By analyzing seismic wave signals, the position, magnitude, and energy of the rock burst can be determined. Therefore, according to the magnitude of microseismic monitoring, the relationship between energy and magnitude can be established, and the scale range of rock burst system can be determined.

$$\Delta U = 10^{1.695M_L+3.18}. \quad (7)$$

$\Delta U$  is the energy released by a rock burst,  $J$ ;  $M_L$  is magnitude.

$$R = \sqrt[3]{\frac{3E(1-\mu) \cdot 10^{1.695M_L+3.18}}{2\pi(10.2\mu^2 - 12.69\mu + 4.49)\gamma^2 H^2}}. \quad (8)$$

### 3. The Working Principle of Liquid CO<sub>2</sub> Fracturing Blasting

**3.1. Structure of CO<sub>2</sub> Cracker.** Liquid CO<sub>2</sub> fracturing blasting technology is mainly used in coal mines to increase the permeability of coal seams and gas extraction efficiency [26, 27]. It is rare to apply liquid CO<sub>2</sub> fracturing blasting technology to rock burst prevention and control. Compared with the traditional explosive technology, the liquid CO<sub>2</sub> fracturing technology has no open fire and can be relatively safe in the process of blasting, and the pressure relief effect is remarkable. The CO<sub>2</sub> cracker is mainly composed of a filling valve, a heating pipe, the main pipe, a sealing gasket, a shearing piece, and an energy release head (Figure 3).

**3.2. The Working Principle of Liquid CO<sub>2</sub> Fracturing Blasting.** When the temperature of liquid CO<sub>2</sub> is lower than 31°C or the pressure is greater than 7.35 MPa, it usually exists in liquid form. When the temperature of liquid CO<sub>2</sub> is higher than 31°C, it begins to gasify. Taking advantage of the phase transition characteristics of CO<sub>2</sub>, liquid CO<sub>2</sub> was filled in the main pipe of the cracker, and the heat pipe was rapidly excited by the detonator. Liquid CO<sub>2</sub> was instantly gasified and expanded to generate high pressure. When the pressure reached the ultimate strength of the constant pressure shearing piece, the shearing piece was broken, and the high-pressure gas was released from the energy release head and then acts on the coal and rock mass, thus realizing the directional fracturing blasting on the coal and rock mass (Figure 4). The crushing zone, fracture zone, and vibration zone were formed successively from the center of the explosion position, so as to complete the pressure relief (Figure 5).

### 4. Test and Research on Liquid CO<sub>2</sub> Fracturing Blasting

**4.1. Test Purpose and Determination of Parameters.** Based on the theory of explosion mechanics, in order to determine the blasting effect of liquid CO<sub>2</sub> fracturing device, reasonable blasting parameters were determined through the experimental research of blasting mechanics. Pressure tests were carried out on the basic parameters of the fracturing blasting in the laboratory to determine the matching relationship between the crackers and borehole diameters, the stress at different positions in the boreholes during the blastings, and the impact on the blasting effect after hole sealing, so as to reveal the controlling mechanism of rock burst of liquid CO<sub>2</sub> fracturing blasting and provide a basis for the prevention and control of rock burst.

The parameters and specifications of liquid CO<sub>2</sub> fracturing blasting test devices are shown in Tables 1 and 2. Different crackers are placed in three different specifications of test devices for blasting test; YE5853-4CH signal amplifier and YE6231 data collector are used in the experiment to collect the pressure of CO<sub>2</sub> released during blasting on the pipe wall, and YE7600 software is used to process the data. Finally, the blasting parameters are determined by comparing and analyzing the pressure data.



FIGURE 3: Structure of CO<sub>2</sub> cracker. 1, filling valve; 2, heating pipe; 3, main pipe; 4, sealing gasket; 5, shearing piece; 6, energy release head.

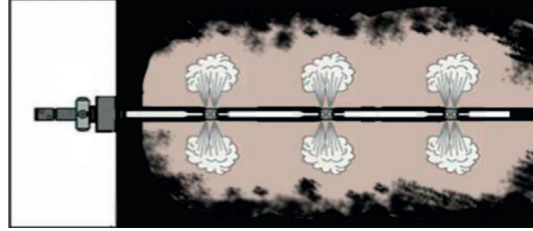


FIGURE 4: Sketch map of working principle of CO<sub>2</sub> cracker.

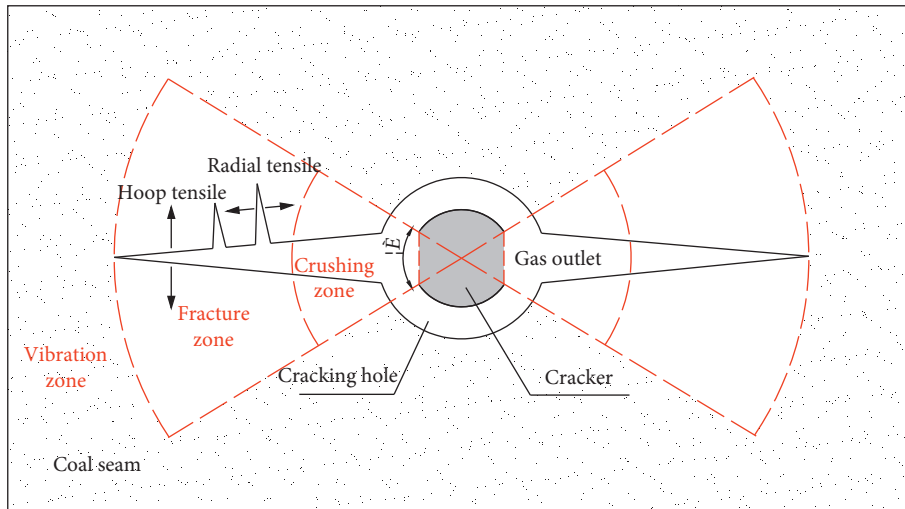


FIGURE 5: Sketch map of damage range of CO<sub>2</sub> cracker.

TABLE 1: Specifications and parameters of test devices.

	Bore (mm)	Length (mm)	Tube thickness (mm)
CSZZ-82/ 2500	82	2500	6.5
CSZZ-68/ 2500	68	2500	4.5
CSZZ-48/ 2500	48	2500	14.0

4.2. *Experiment Scheme and Design.* According to the purpose of the experiment, different specifications of crackers were selected and put into three different specifications of test devices for blasting test. Six experiment schemes were designed, and each scheme was tested three times. The design of the experiment scheme is shown in Table 3.

Before blasting, all the small holes in the pipe wall were opened, and the blasting power was controlled by controlling the strength of the shearing pieces. Sampling

frequency was set to 96 kHz, and pure cotton cloth was used to seal holes when the holes needed to be sealed. Force tests at different positions of the test device are shown in Figure 6.

4.3. *Analysis of Experiment Data.* According to the experimental schemes of liquid CO<sub>2</sub> fracturing blasting, ZLQ-38/300 was selected to blast in CSZZ-82/2500, and the strength of shearing piece in the cracker was 300 MPa. Four sensors were installed to test the force at different positions: the pressure sensor at point A is about 21 mm away from the energy release head of the cracker, which keeps level with the venting of the energy release head; the measuring points B and C were located at the top of the testing device, and the measuring point D was located at the tail of the testing device. The stress test data of different positions after liquid CO<sub>2</sub> blasting are shown in Figure 7.

Through the liquid CO<sub>2</sub> fracturing blasting test, it can be seen that the pressure at point A was the largest, and the pressure was above 200 MPa, which could meet the requirement of coal failure; the pressure at measuring points B,

TABLE 2: Specifications and parameters of liquid CO<sub>2</sub> crackers.

	Bore (mm)	Length of main pipe (mm)	Cartridge length (mm)	Material of shearing piece	Strength of shearing piece (MPa)	CO <sub>2</sub> capacity (kg)
ZLQ-38/300	38	300	15	High strength alloy steel	200/300	0.234
ZLQ-38/600	38	600	15	High strength alloy steel	200/300	0.468

TABLE 3: Experiment schemes design.

Schemes	Specifications of test devices	Specifications of crackers	Sealed or not sealed	Number of sensors	Strength of shearing piece (MPa)	Spacing between hole wall and energy release head (mm)
No. 1	CSZZ-82/2500	ZLQ-38/300	Sealed	4	300	21
No. 2	CSZZ-82/2500	ZLQ-38/300	Sealed	2	300	21
No. 3	CSZZ-82/2500	ZLQ-38/300	No	2	300	21
No. 4	CSZZ-82/2500	ZLQ-38/300	Sealed	2	200	21
No. 5	CSZZ-68/2500	ZLQ-38/300	Sealed	2	200	17
No. 6	CSZZ-48/2500	ZLQ-38/300	Sealed	2	200	10

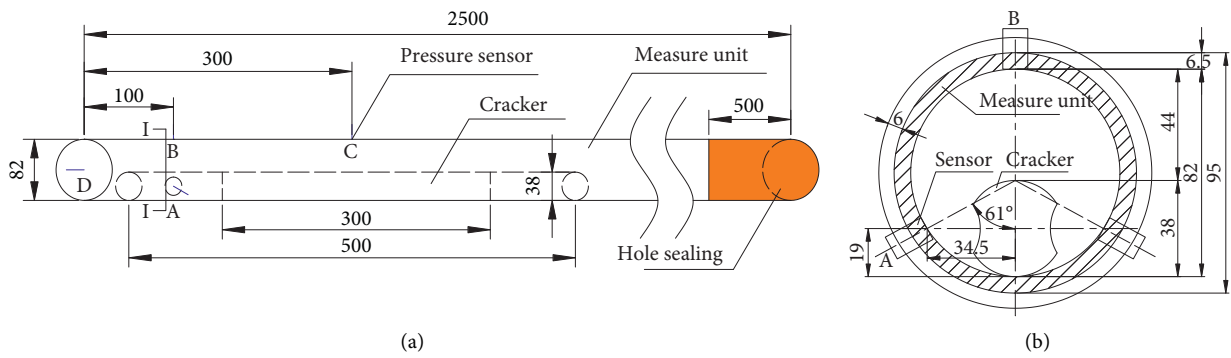
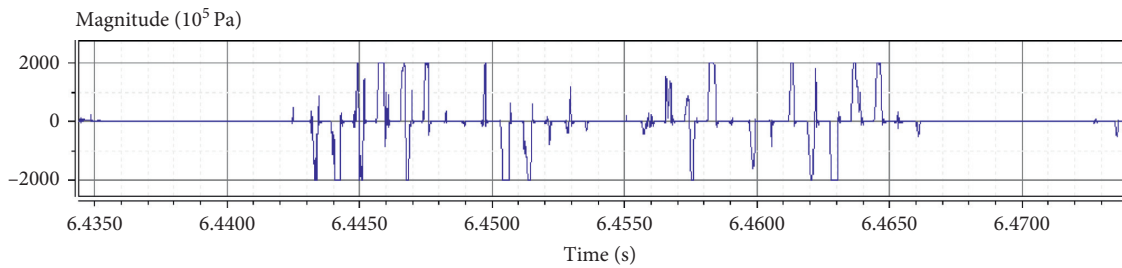
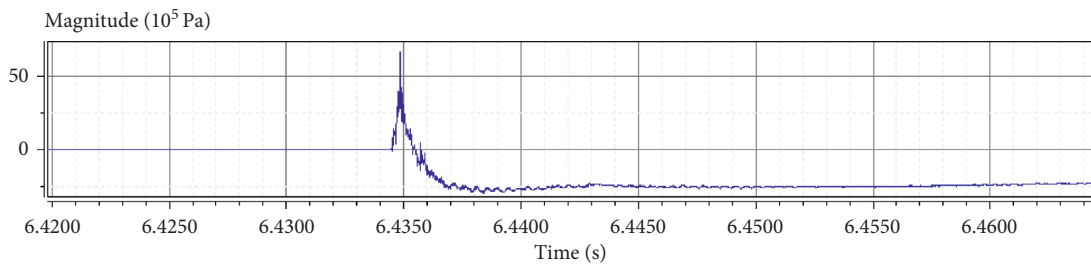


FIGURE 6: Diagram of force tests at different positions (length unit: mm).



(a)



(b)

FIGURE 7: Continued.

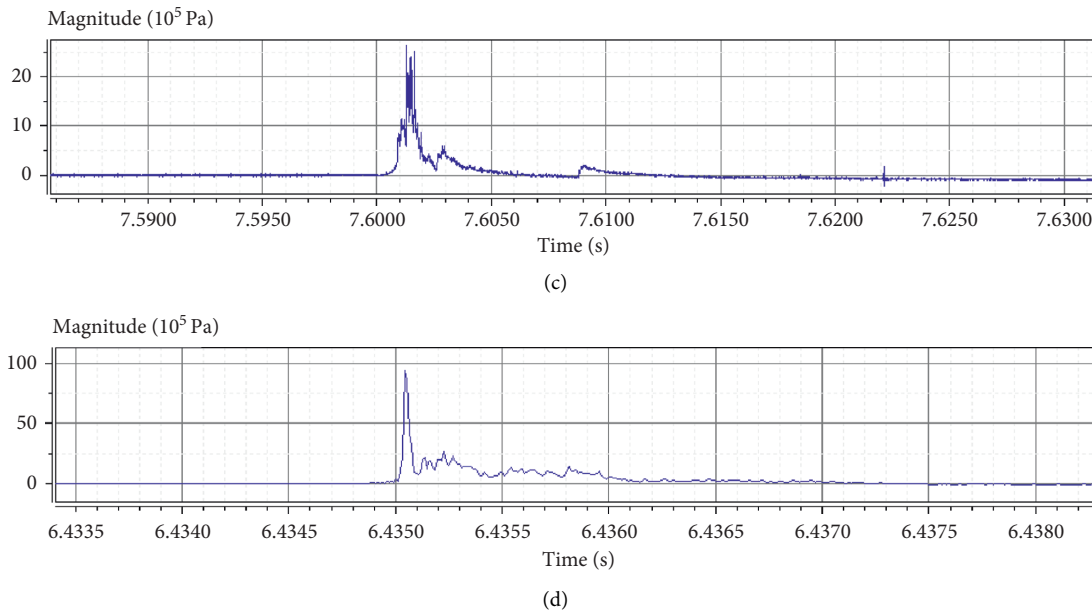


FIGURE 7: Waveforms of stress in different positions of CO<sub>2</sub> fracturing blasting. (a) The waveform of measuring point A (201.3 MPa). (b) The waveform of measuring point B (6.6 MPa). (c) The waveform of measuring point C (2.6 MPa). (d) The waveform of measuring point D (9.4 MPa).

C, and D was no more than 10 MPa, which did not meet the requirement of coal failure. Therefore, in the practice, the energy release head of the cracker should be directed to the risk relief area, and the radial level of the energy release head of the cracker must be maintained. It is suggested that the distance between the hole wall and the energy release head should be between 10 mm and 15 mm. For the area with a longer blasting range, multisection series blasting can be implemented.

## 5. Analysis of CO<sub>2</sub> Fracturing Blasting of Rock Burst System in Jixian Coal Mine

**5.1. Analysis of Rock Burst System in Jixian Coal Mine.** The rock burst in Jixian Coal Mine is serious, especially in the syncline axis of the No. 2 mining area in the deep mining area, where gas content is high, and multiple rock bursts occur continuously. The magnitude of rock burst monitored by microseism in the mine is mostly within the range of  $M_L = 0.5-2.5$ . On March 11, 2013, a rock burst with the magnitude of 1.5 occurred in the lower roadway of the left first working face in West No. 2 Mining Area. The rock burst caused the floor heave of the 15 m roadway outward from the coal wall of the working face. The range of 210 m to 270 m of the lower roadway was seriously damaged by the impact, and the adjacent working faces were all shocked. The rock burst location was vertically depth of  $h = 700$  m from the surface, and the lithology of the floor was sandstone,  $E = 21700$  MPa, and  $\mu = 0.24$ . According to formulas (5) and (6), the energy released by the “3.11” rock burst system in Jixian Coal Mine was  $\Delta U = 5.3 \times 10^5$  J, and the radius of the rock burst system is 25.9 m (Figure 8).

When a rock burst occurs, after a period of energy transfer, exchange, supplement, and storage of the rock burst system, the energy reaches the critical energy of the next rock burst, and the rock burst will occur again under the influence of mining engineering. Therefore, in view of the “3.11” rock burst system of Jixian Coal Mine, the liquid CO<sub>2</sub> fracturing blasting method is chosen as the priority to relieve the pressure of rock burst system.

**5.2. Analysis of CO<sub>2</sub> Fracturing Blasting Technology for Rock Burst System.** According to the theoretical analysis of liquid CO<sub>2</sub> fracturing blasting and laboratory experiment results, multiple series blasting was carried out with crackers with specifications of ZLQ-38/300 and ZLQ-38/600. The weight of injected CO<sub>2</sub> was 0.17 kg and 0.26 kg, respectively, the diameter of the borehole was 50 mm, a total of 5 boreholes were constructed, the drilling spacing was 10 m, and the distance between the cracker and the borehole wall was 12 mm. Hole collapse occurred in the borehole after blasting. There were many broken coal blocks and the hole wall was rough, which contributed to the pressure relief for the rock burst pressure system (Figure 9).

The application of liquid CO<sub>2</sub> fracturing blasting technology in the prevention and control of rock burst in Jixian Coal Mine shows that CO<sub>2</sub> fracturing blasting reduces the stress concentration of rock burst system and transfers energy to the deeper part, and there is no open fire in blasting. It is a new, safe, and efficient technology to prevent rock burst, which can be applied widely.

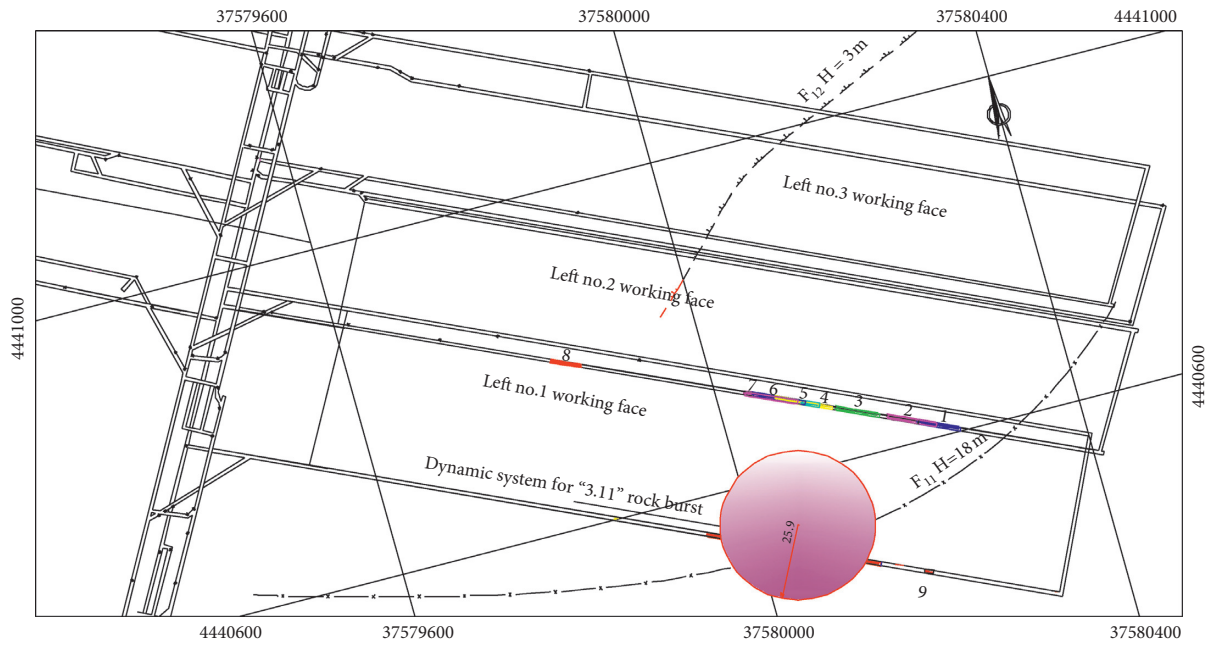


FIGURE 8: Dynamic system for "3.11" rock burst in Jixian Coal Mine.

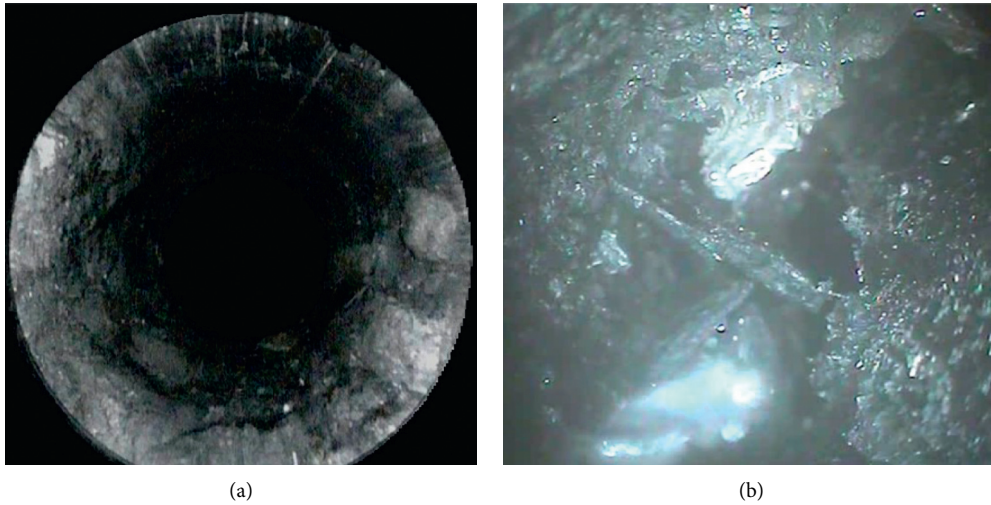


FIGURE 9: Borehole surface before and after liquid  $\text{CO}_2$  fracturing blasting. (a) Before blasting. (b) After blasting.

## 6. Conclusions

- (1) It is difficult to accurately predict the "time, space, and intensity" of rock burst, but the possibility of rock burst can be predicted according to the results of microseismic monitoring. The relationship between rock burst and monitoring data of mine microseism is established.
- (2) The stress field of rock burst mine is mostly horizontal compression tectonic stress field. The rock burst system under the tectonic stress field is established. The energy criterion related to mining depth, system size, and medium properties of coal and rock mass is analyzed, and the critical energy condition is proposed.
- (3) According to the magnitude of microseismic monitoring, the relationship between the energy of rock burst and the radius of rock burst system is determined. It is revealed that the failure process of rock burst system is a nonlinear dynamic process of accumulating energy in stable state and releasing energy in unstable state.

- (4) The application of liquid CO<sub>2</sub> fracturing blasting technology in the prevention and control of “3.11” rock burst in Jixian Coal Mine shows that the application of liquid CO<sub>2</sub> fracturing blasting in the rock burst system reduces the stress concentration of the rock burst system and makes the energy transfer to the deeper part, and there is no open fire in the blasting process, which has a good pressure relief effect. It can be applied widely in the prevention and control of rock burst in coal mines.

## Data Availability

The experimental data used to support the findings of this study are included within the article.

## Conflicts of Interest

The authors declare no potential conflicts of interest with respect to the research, authorship, and/or publication of this article.

## Acknowledgments

This research was funded by the Research Fund of Key Laboratory of Mining Disaster Prevention and Control (MDPC201926), the State Key Research Development Program of China (2017YFC0804209), and the National Natural Science Foundation of China (51604139).

## References

- [1] H. Xie, J. Wang, G. Wang et al., “New ideas of coal revolution and layout of coal science and technology development,” *Journal of China Coal Society*, vol. 43, no. 5, pp. 1187–1197, 2018.
- [2] C. Fan, S. Li, D. Elsworth, J. Han, and Z. Yang, “Experimental investigation on dynamic strength and energy dissipation characteristics of gas outburst-prone coal,” *Energy Science & Engineering*, vol. 8, no. 4, pp. 1015–1028, 2020.
- [3] Q. Qi, H. Li, Z. Deng, S. Zhao et al., “Studying of standard system and theory and technology of rock burst in domestic,” *Coal Mining Technology*, vol. 22, no. 01, pp. 1–5, 2017.
- [4] L. Dou, “Induced shock and control of hard roof,” in *Proceedings of the 37th International Conference on Ground Control in Mining*, China, Xuzhou, July 2018.
- [5] T. Lan, C. Fan, H. Zhang et al., “Seepage law of injected water in the coal seam to prevent rock burst based on coal and rock system energy,” *Advances in Civil Engineering*, vol. 2018, Article ID 8687108, 9 pages, 2018.
- [6] Y. Pan, “Integrated study on compound dynamic disaster of coal-gas outburst and rockburst,” *Journal of China Coal Society*, vol. 41, no. 01, pp. 105–112, 2016.
- [7] Y. Jiang, Y. Pan, F. Jiang, L. Dou, and Ju Yang, “State of the art review on mechanism and prevention of coal bumps in China,” *Journal of China Coal Society*, vol. 39, no. 2, pp. 205–213, 2014.
- [8] Q. Qi, Z. Ouyang, H. Shankun, H. Li, X. Li, and N. Zhang, “Study on types of rock burst mine and prevention methods in China,” *Coal Science and Technology*, vol. 42, no. 10, pp. 1–5, 2014.
- [9] Y. Jiang and Y. Zhao, “State of the art: investigation on mechanism, forecast and control of coal bumps in China,” *Chinese Journal of Rock Mechanics and Engineering*, vol. 34, no. 11, pp. 2188–2204, 2015.
- [10] T. Lan, H. Zhang, J. Han, and W. Song, “Study on the rockburst mechanism based on geo-stress and rock mass energy principle,” *Journal of Mining & Safety Engineering*, vol. 29, no. 06, pp. 840–844, 2012.
- [11] Z. Ma, R. Gu, Z. Huang, G. Peng, L. Zhang, and D. Ma, “Experimental study on creep behavior of saturated disaggregated sandstone,” *International Journal of Rock Mechanics and Mining Sciences*, vol. 66, pp. 76–83, 2014.
- [12] M. Birk, R. Dapp, N. V. Ruitter, and J. Becker, “GPU-based iterative transmission reconstruction in 3D ultrasound computer tomography,” *Journal of Parallel and Distributed Computing*, vol. 74, no. 1, pp. 1730–1743, 2014.
- [13] Y. Ju, J. Zheng, M. Epstein, L. Sudak, J. Wang, and X. Zhao, “3D numerical reconstruction of well-connected porous structure of rock using fractal algorithms,” *Computer Methods in Applied Mechanics and Engineering*, vol. 279, pp. 212–226, 2014.
- [14] H. Zhao, L. Yang, Li Kun, and Y. Zhao, “Design and experimental research of a multifunctional loading system based on industrial CT,” *Machine Tool and Hydraulics*, vol. 46, no. 4, pp. 109–115, 2018.
- [15] L. Dong, J. Wesseloo, Y. Potvin, and X. Li, “Discrimination of mine seismic events and blasts using the Fisher classifier, naive bayesian classifier and logistic regression,” *Rock Mechanics and Rock Engineering*, vol. 49, no. 1, pp. 183–211, 2016.
- [16] F. Gan, X. Wang, M. Wang, and Y. Kang, “Experimental investigation of thermal cycling effect on fracture characteristics of granite in a geothermal-energy reservoir,” *Engineering Fracture Mechanics*, vol. 235, Article ID 107180, 2020.
- [17] G. Bai, X. Zeng, X. Li, X. Zhou, Y. Cheng, and J. Linghu, “Influence of carbon dioxide on the adsorption of methane by coal using low-field nuclear magnetic resonance,” *Energy & Fuels*, vol. 34, no. 5, pp. 6113–6123, 2006.
- [18] V. Frid, “Rockburst hazard forecast by electromagnetic radiation excited by rock fracture,” *Rock Mechanics and Rock Engineering*, vol. 30, no. 4, pp. 229–236, 1997.
- [19] M. Alber, R. Fritschen, M. Bischoff, and T. Meier, “Rock mechanical investigations of seismic events in a deep longwall coal mine,” *International Journal of Rock Mechanics and Mining Sciences*, vol. 46, no. 2, pp. 408–420, 2009.
- [20] M. Geng, Z. Ma, P. Gong et al., “Analysis of the effect on pressure relief by the pressure relieving hole layouts on high stress coal roadway,” *Journal of Safety Science and Technology*, vol. 11, pp. 5–10, 2012.
- [21] C. Fan, M. Luo, S. Li, H. Zhang, Z. Yang, and Z. Liu, “A thermo-hydro-mechanical-chemical coupling model and its application in acid fracturing enhanced coalbed methane recovery simulation,” *Energies*, vol. 12, no. 4, p. 626, 2019.
- [22] Z. Ouyang, “Application and mechanism of mine strata pressure pumping prevention with multi-stage blasting pressure releasing technology,” *Coal Science and Technology*, vol. 10, pp. 32–36, 2014.
- [23] P. Konicek, K. Soucek, L. Stas, and R. Singh, “Long-hole destress blasting for rockburst control during deep underground coal mining,” *International Journal of Rock Mechanics and Mining Sciences*, vol. 61, pp. 141–153, 2013.
- [24] T. Lan, C. Fan, S. Li et al., “Probabilistic prediction of mine dynamic disaster risk based on multiple factor pattern recognition,” *Advances in Civil Engineering*, vol. 2018, Article ID 7813931, 6 pages, 2018.

- [25] J. Liu, L. Xie, Y. Yao, Q. Gan, P. Zhao, and L. Du, "Preliminary study of influence factors and estimation model of the enhanced gas recovery stimulated by carbon dioxide utilization in shale," *ACS Sustainable Chemistry & Engineering*, vol. 7, no. 24, pp. 20114–20125, 2019.
- [26] C. Fan, D. Elsworth, S. Li, L. Zhou, Z. Yang, and Y. Song, "Thermo-hydro-mechanical-chemical couplings controlling CH<sub>4</sub> production and CO<sub>2</sub> sequestration in enhanced coalbed methane recovery," *Energy*, vol. 173, pp. 1054–1077, 2019.
- [27] X. Zhou, J. Men, D. Song et al., "Research on increasing coal seam permeability and promoting gas drainage with liquid CO<sub>2</sub> blasting," *China Safety Science Journal*, vol. 02, pp. 60–65, 2015.